Assessing Motor Topologies

By Steve Mowry

The underhung voice coil topology is universally considered to be the most linear motor topology implementation with respect to displacement. This is where the magnetic gap height is greater than the voice coil wind height by definition. There are, however, reasonable limits on how tall the magnetic gap can be relative to how short the voice coil can be, especially in smaller transducers. The more commonly utilized overhung topology is then defined as the voice coil wind being taller than the magnetic gap height. This works relatively well but is inherently nonlinear and has mass and wind height trade-off limits.

Recently, there have been some interesting hybrid and/or compound motor topologies introduced. These include LMS, BLX^2, and LRRP. An interesting alternative to these proprietary hybrid motor topologies, based on Burton A. Babb's US Patent 3,983,337 filed June 21, 1973 has the potential to facilitate very high linear displacement when applied to a decade old design using familiar tall gap motor topology.

The voice coil is really a flux density integrator with respect to its surface formed by the radius, *dr* and the wind height, *dx*. Starting with Gauss's Law as it applies to the voice coil's radial surface, equation 1 illustrates the relationship between DC flux and flux density, B, where Φ is the DC magnetic flux, Tm^2.

$$\Phi(x)=\int\int B(x)2\pi drdx \ Tm^2 \qquad (1)$$

where: $dl = N2\pi dr$ and N is the number of turns, m (2)
Substituting and simplifying: $N\Phi(x) = \int Bl(x)dx \ Tm^2$ (3)
*N*Φ is the DC flux linkage, sometimes referred to as Δ. Taking the derivative of both sides of equation 3, the result is shown in equation 4.

$$B1(x) = \frac{d\Delta(x)}{dx} Tm \qquad (4)$$

Equation 4 shows that Bl(x) varies with position and is defined as the change in flux linkage relative to the wind height of the voice coil.

The value of Bl(x) is really random in nature and can be evaluated based on the probability of where the voice coil is. Thus I have approximated the behavior of each motor topology using exponential functions that are in the form of probability density functions. I know the system, but I don't quite know the input. The value of Bl(x) changes with voice coil position, but I don't know exactly where the voice coil is. However, if the Bl(x) function approaches a constant, Bl(0), then I simply don't care where the voice coil is, as long as it is between –X and X.

The following relates to the DC flux linkage characteristics of several voice coils within several similar motor topologies.

OVERHUNG COIL

Figure 1 is an example of overhung voice coil topology. The Bl(x) function for the overhung topology is nonlinear and resembles an inverted parabolic type function. Equation 5 is a generalized first order approximation of this phenomenon and is in the form of a probability density function, where m and n are constants related to the magnetic gap and voice coil geometries and e is Euler's number.

$$B1(x) \approx B1(0)e^{-mx2n} \ Tm \qquad (5)$$

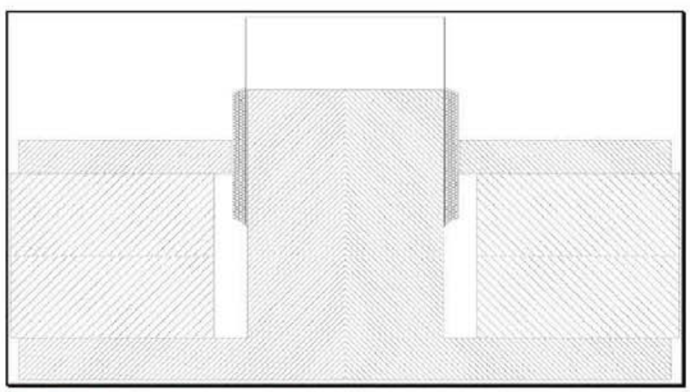

FIGURE 1: Sectional illustration of a highly overhung voice coil motor topology.

WELLHUNG COIL

I used the wellhung topology for subwoofer designs back in the late 1990s. Relative to the highly overhung motor topology in ***Fig. 1***, the gap is tall and the voice coil is also tall. In this case the voice coil wire was aluminum to keep moving mass at a reasonable value for such a tall voice coil. The peak value of Bl is typically reduced by the aluminum relative to copper wire, but the tall gap and tall voice coil result in high flux linkage at or about the rest position (***Fig. 2***).

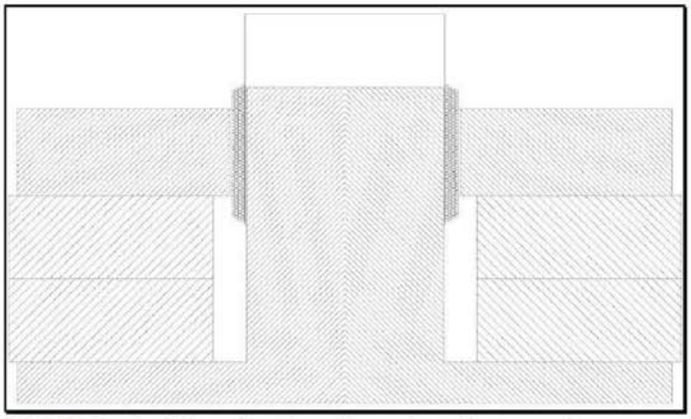

FIGURE 2: Sectional illustration of a wellhung voice coil motor topology.

This is the most efficient motor topology but also the most nonlinear of the topologies discussed here. The wellhung topology was a favorite with competition car audio and dB Drags several years ago. With the development of the Klippel DA, the industry focus shifted to the nonlinear parameters, including Bl(x) and linearity based X_{max} limits. ***Figure 3*** is a decade-old wellhung low-frequency transducer implementation.

The following topologies can be designed to be linear with respect to displacement in a large signal sense.

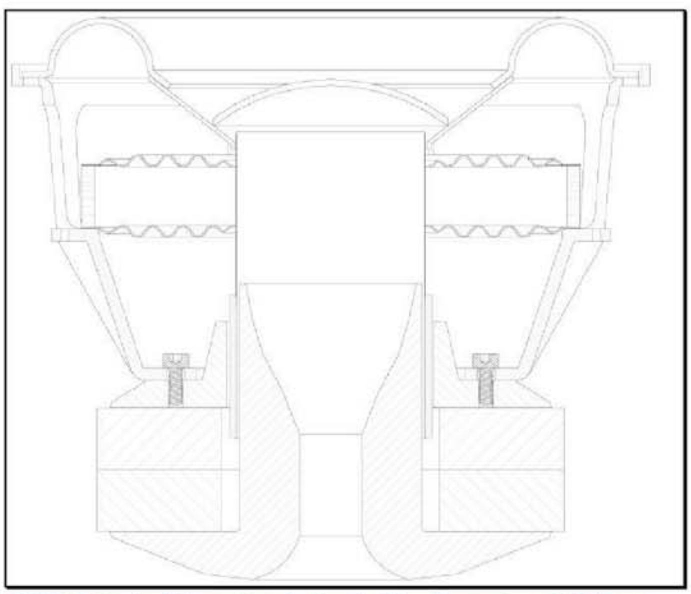

FIGURE 3: Sectional illustration of a decade-old wellhung voice coil 10" transducer assembly.

VARIABLE DENSITY COIL

A solution to the overhung nonlinearity is to wind the voice coil nonlinearly. This is shown in equation 6 and ***Fig. 4***. The voice coil winding density is increased exponentially from the center of wind in both the positive and negative directions (www.

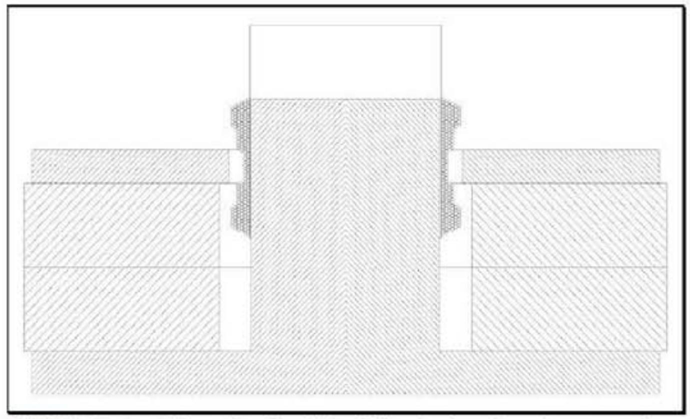

FIGURE 4: Sectional illustration of variable winding density voice coil motor topology.

audiopulse.com/products/technologies/lms/) to compensate for the exponential Bl decay resulting from displacement of the coil from the rest position, x = 0.

$$B1(x) \approx B1(0)e^{mx2n}\, e^{-mx2n}\, Tm \qquad (6)$$

$$B1(x) \approx B1(0);\ -X>x>X$$

A problem with this solution is that the voice coil becomes massive with a wide peak cross-section at the end limits that requires a wide magnetic gap. It seems better suited for large subwoofers that are less sensitive to moving mass requirements and motor assemblies can be made large. A wide gap and a massive voice coil will certainly impact transducer sensitivity.

UNDERHUNG COIL

The underhung voice coil motor topology is a proven solution, and an example illustrated in ***Fig. 5*** and equation 7 shows that the flux linkage is inherently constant over a displacement range. It is linear for a range of displacement, then the Bl(x) value falls exponentially.

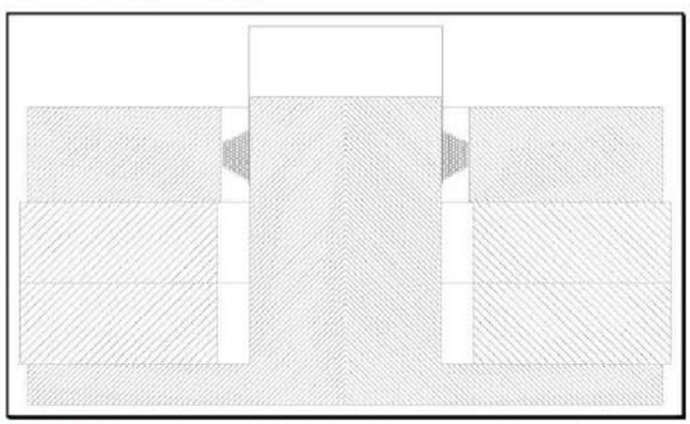

FIGURE 5: Sectional illustration of underhung voice coil motor topology.

$$B1(x) \approx B1(0); -X<x<X \text{ Tm} \quad (7)$$
$$B1(x) \approx B1(0)e^{-m(|x|-X)2n}; -X \geq x \geq X$$

Equation 8 shows the linear displacement limit guidelines for the following overhung topologies including wellhung and nonlinear wound voice coil and the underhung topology, where h is the voice coil wind height and g is the magnetic gap height, the difference between the gap and coil heights.

$$X = \frac{|g-h|}{2}\text{m} \quad (8)$$

XBL^2

XBL^2 is a clever hybrid dual gap underhung/overhung voice coil motor implementation. It does require secondary CNC machining of the pole and multiple top plates. At and about the rest position, the voice coil links to the two gaps and is underhung by definition, gap taller than coil wind height, but as the coil is displaced into and out of the motor assembly, the coil becomes overhung with regard to each of the two-segmented gaps.

It is convenient to place a heavy aluminum shorting ring between the two gaps. This has been shown to be effective in reducing inductance related nonlinearity, Le(x,*i*) and the AC *Bl*(x,*i*).

LRRP

The XBL^2 and STEP's Low Reluctance Return Path (LRRP) topologies are very similar in function, but the LRRP is a more complex and physically larger implementation and can provide very high Bl due to the arraying of magnets. XBL^2 and LRRP both utilize two gaps with one coil positioned between those gaps. They make efficient use of the voice coil wind height—see equation 10 where d_g is the distance between the gaps. Bl(x) can be made linear over a range, -X to X, with the careful selection of appropriate geometry as equation 9 indicates.

$$B1(x) \approx B_1 1(0)e^{-m(x-X)2n} + B_2 1(0)e^{-m(x+X)2n} \text{ Tm} \quad \mathbf{(9)}$$
$$B1(x) \approx B1(0); -X > x > X$$

$$X \approx \frac{h+d_g}{2}\text{m} \quad \mathbf{(10)}$$

where the height of the voice is less than the total gap height, h < g.

SDVC

Another simple solution to the nonlinearity of the overhung coil is to reduce the peak flux linkage by removing voice coil turns where the peak values occur, at and about the zero or center of the winding position (***Fig. 8***). XBL^2 and LRRP also do this by segmenting the gap into two effective gaps. The result for the SDVC can be approximated as two nonlinear functions each with a linear wound (constant density) voice coil summed to a linear function over a range, the Symmetrical Dual Voice

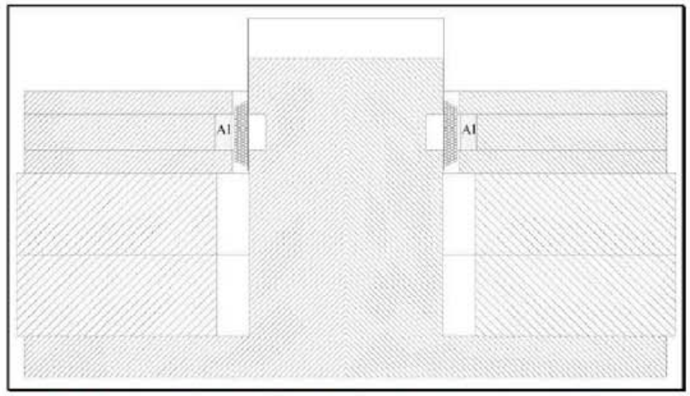

FIGURE 6: Sectional illustration of BLX2 voice coil motor topology with shorting ring.

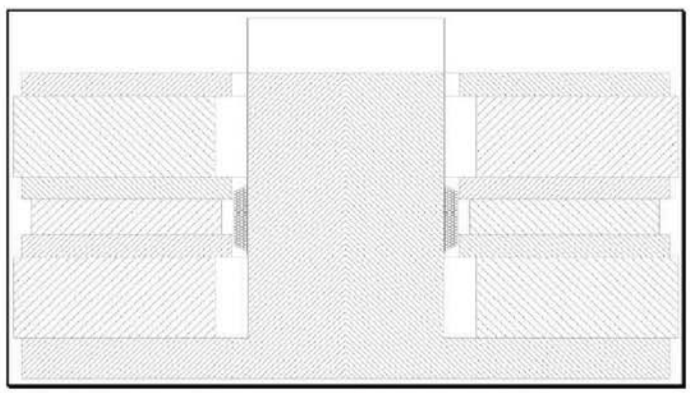

FIGURE 7: Sectional illustration of LRRP voice coil motor topology.

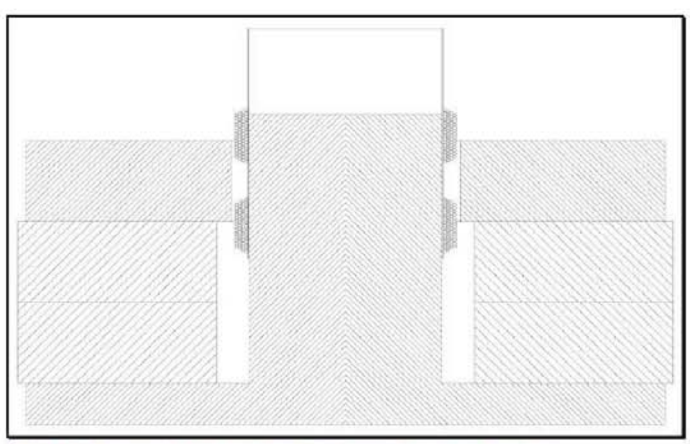

FIGURE 8: Sectional illustration of SDVC voice coil motor topology.

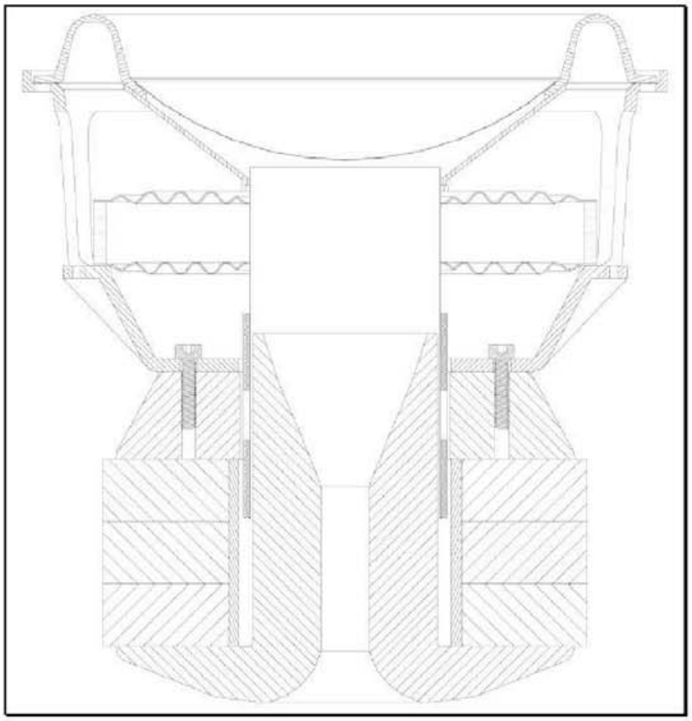

FIGURE 9: Sectional illustration of a 3″ nominal diameter voice coil SDVC updated 10″ WOW transducer assembly.

DC Resistance@25C	=	3.69	Ω	Conductor OD	0.0224 in
Conductor Length	=	1328.3	in		
V C Section Width	=	0.0895	in	Insulated Wire OD	0.0246 in
Voice Coil Outside Dia	=	2.1535	in		
Voice Coil Avg. Dia	=	2.0650	in	Bobbin Glue Thick	0.0010 in
Wind Inside Diameter	=	1.9765	in		
Number of Turns	=	204.7		Bobbin Thick	0.0030 in
Turns on 1st Layer	=	52.7			
Stacking Factor	=	0.679		Packing Factor	0.948
Inner Wind Height	=	1.367	in		
Outer Wind Height	=	1.289	in	DC Resistance@25C	3.69 Ω
Average Wind Height	=	1.328	in		
Total Wire Mass	=	23.27	g	No. of Layers	4
Adhesive Mass	=	2.34	g		
Total Mass w/o Bobbin	=	25.61	g	Voice Coil ID	1.9685 in
					TYPE RHO
				Round Wire	AL 1.0948 E-6

FIGURE 10: Wellhung voice coil model.

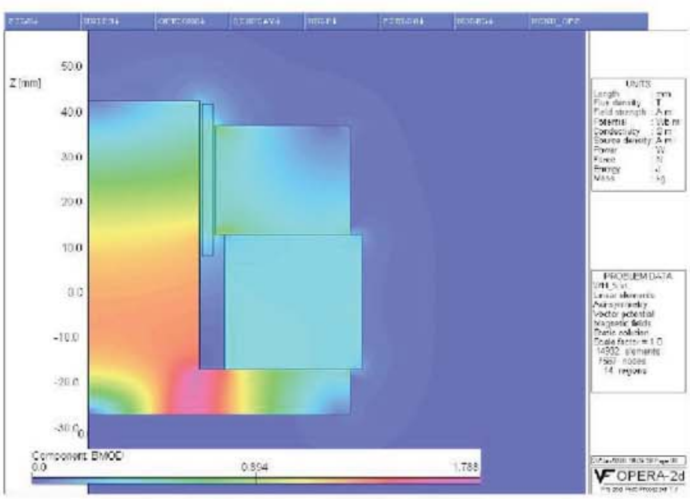

FIGURE 11: Contour plot of the simulation of the magnitude of the DC flux density, |B|, for the wellhung motor assembly model.

Coil (SDVC). The dashed traces in ***Fig. 22*** have complementary direction decays (rolloffs) that are quite linear and symmetrical about x = 0. This works like a flux linkage crossover between the two voice coils as shown in equation 11.

The SDVC topology can utilize an aluminum shorting ring on the magnets' ID and an aluminum basket can function as a shorting ring on the top side of the gap plate. Ironically, this is also the dual of the single shorting ring between the two effective XBL^2's gaps. This is shown in the illustration of an SDVC update example in ***Fig. 9.***

$$B1(x) \approx B11(0)e^{-m(x+X)2n} + B12(0)e^{-m(x-X)2n} \ Tm \quad (11)$$
$$B1(x) \approx B1(0); -X > x > X$$

A linear displacement limit guideline for the SDVC topology is shown by equation 12.

$$X \approx \frac{g+d_c}{2} m \quad (12)$$

where the height of one coil is less than the gap height, $h_1 < g$.

d_c is the spacing between coils and the wind height of one coil is h_1. The SDVC makes good use of the gap height as does the underhung topology. The value of X is then obtained from simulation and subsequently verified with a Klippel DA.

Utilizing three coil segments is an option, where extreme linear displacement is the target. However, the trade-offs are the same, Bl(0) for X_{max} and a three-segment implementation would require a very large motor assembly in a tall package.

SIMULATIONS

I will perform a virtual experiment. I will simulate an XBL^2 motor assembly, then, using the same magnets and basic topology, I will reconfigure the voice coil used in the XBL^2 simulation from a 4-layer to an 8-layer and simulate an underhung motor assembly. Then I will simulate the wellhung and the SDVC topology using 4-layer aluminum wire voice coils and then plot all results. I will maintain constant clearances around the voice coil(s). ***Figures 10*** through ***21*** contain the voice coil models and contour plots of the DC magnetic simulations including contour plots of the magnitude of the flux density, |B|, and the flux distribution (flux lines).

Figure 10 contains the wellhung voice coil model.

The information from the voice coil models is used within the $d\Lambda(x)/dx$ command file that performs a voice coil sweep through the magnetic gap inside the finite element model. The results are plotted in ***Fig. 22***.

The contour plots of simulations in ***Figs. 11*** and ***12*** illustrate the wellhung or mildly overhung voice coil links to most of the gap flux at the rest position. ***Figure 13*** contains the voice coil model for one coil of the SDVC. ***Figure 16*** contains the short underhung voice coil model.

Figures 17 and ***18*** illustrate that the underhung voice coil is within a uniform DC flux density just as long as the coil remains within the gap. ***Figure 19*** contains the XBL^2 voice coil model.

The simulations of flux density illustrated in ***Fig. 20*** and the flux distribution in ***Fig. 21*** clearly shows that the XBL^2 has two magnetic gaps spaced by some distance, d_g.

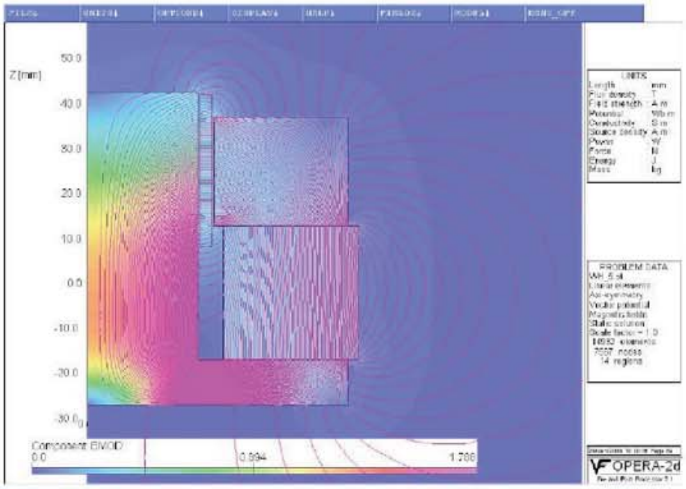

FIGURE 12: Contour plot of the simulation of the DC flux distribution for the wellhung motor assembly model.

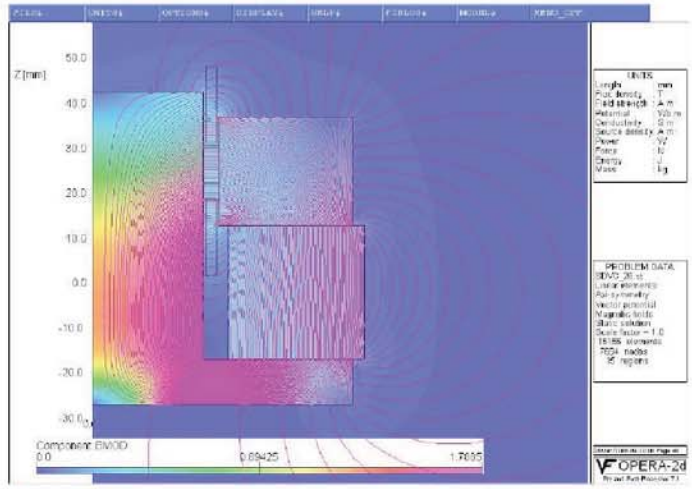

FIGURE 15: Contour plot of the simulation of the DC flux distribution for the SDVC motor assembly model.

DC Resistance@25C	= 1.85 Ω	Conductor OD	0.0224 in
Conductor Length	= 865.9 in		
V C Section Width	= 0.0895 in	Insulated Wire OD	0.0246 in
Voice Coil Outside Dia	= 2.1535 in		
Voice Coil Avg. Dia	= 2.0650 in	Bobbin Glue Thick	0.0010 in
Wind Inside Diameter	= 1.9765 in		
Number of Turns	= 102.7	Bobbin Thick	0.0030 in
Turns on 1st Layer	= 27.2		
Stacking Factor	= 0.679	Packing Factor	0.948
Inner Wind Height	= 0.705 in		
Outer Wind Height	= 0.627 in	DC Resistance@25C	1.85 Ω
Average Wind Height	= 0.666 in		
Total Wire Mass	= 11.67 g	No. of Layers	4
Adhesive Mass	= 1.17 g		
Total Mass w/o Bobbin	= 12.84 g	Voice Coil ID	1.9685 in
			TYPE RHO
		Round Wire	AL 1.0948 E-6

FIGURE 13: Half SDVC voice coil model.

DC Resistance@25C	= 3.69 Ω	Conductor OD	0.0151 in
Conductor Length	= 975.8 in		
V C Section Width	= 0.1204 in	Insulated Wire OD	0.0169 in
Voice Coil Outside Dia	= 2.2152 in		
Voice Coil Avg. Dia	= 2.0959 in	Bobbin Glue Thick	0.0010 in
Wind Inside Diameter	= 1.9765 in		
Number of Turns	= 148.2	Bobbin Thick	0.0030 in
Turns on 1st Layer	= 22.0		
Stacking Factor	= 0.668	Packing Factor	0.948
Inner Wind Height	= 0.393 in		
Outer Wind Height	= 0.268 in	DC Resistance@25C	3.69 Ω
Average Wind Height	= 0.330 in		
Total Wire Mass	= 25.48 g	No. of Layers	8
Adhesive Mass	= 0.72 g		
Total Mass w/o Bobbin	= 26.19 g	Voice Coil ID	1.9685 in
			TYPE RHO
		Round Wire	Cu 6.7716 E-7

FIGURE 16: Underhung voice coil model.

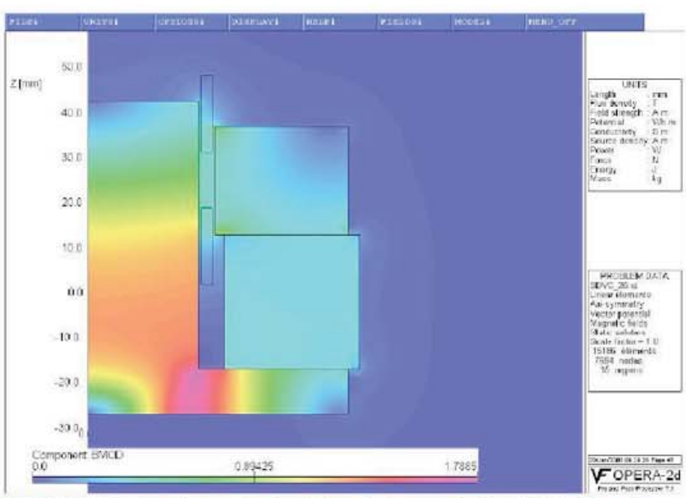

FIGURE 14: Contour plot of the simulation of the magnitude of the DC flux density, |B|, for the SDVC motor assembly model.

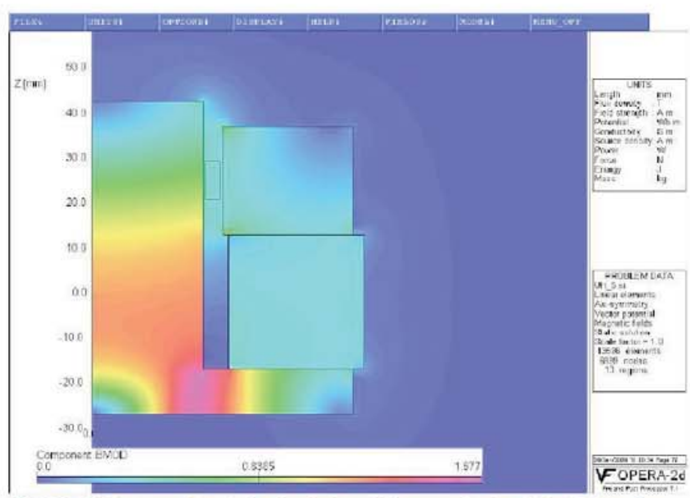

FIGURE 17: Contour plot of the simulation of the magnitude of the DC flux density, |B|, for the underhung motor assembly model.

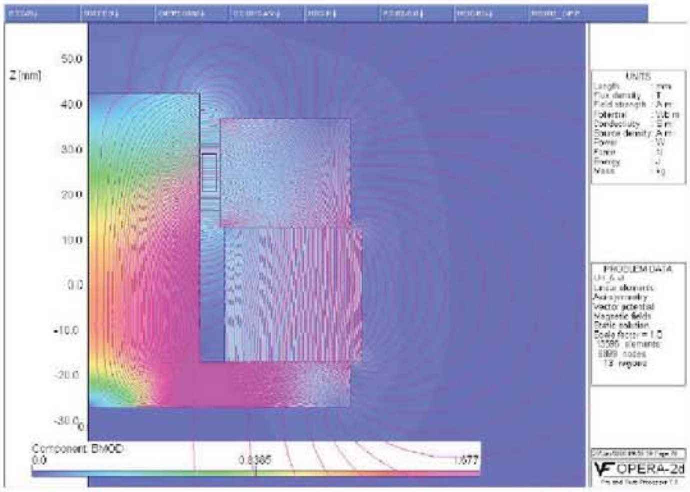

FIGURE 18: Contour plot of the simulation of the DC flux distribution for the underhung motor assembly model.

DC Resistance@25C	= 3.69 Ω	Conductor OD	0.0151 in	
Conductor Length	= 969.4 in			
V C Section Width	= 0.0619 in	Insulated Wire OD	0.0169 in	
Voice Coil Outside Dia	= 2.0983 in			
Voice Coil Avg. Dia	= 2.0374 in	Bobbin Glue Thick	0.0010 in	
Wind Inside Diameter	= 1.9765 in			
Number of Turns	= 151.5	Bobbin Thick	0.0030 in	
Turns on 1st Layer	= 39.4			
Stacking Factor	= 0.644	Packing Factor	0.948	
Inner Wind Height	= 0.703 in			
Outer Wind Height	= 0.649 in	DC Resistance@25C	3.69 Ω	
Average Wind Height	= 0.676 in			
Total Wire Mass	= 25.14 g	No. of Layers	4	
Adhesive Mass	= 0.83 g			
Total Mass w/o Bobbin	= 25.97 g	Voice Coil ID	1.9685 in	
			TYPE	RHO
		Round Wire	Cu	6.7716 E-7

FIGURE 19: XBL2 voice coil model.

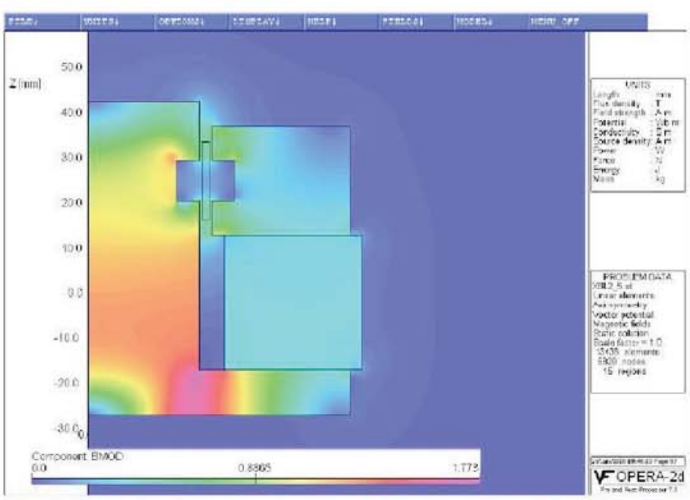

FIGURE 20: Contour plot of the simulation of the magnitude of the DC flux density, |B|, for the SBL2 motor assembly model.

The DC resistance and the mass are essentially identical for all voice coil models along with the magnets and the pole and the gap plates being essentially the same within the finite element models. The curves in ***Fig. 22*** could be moved up or down by increasing or decreasing magnet size and perhaps the back plate could be thickened if the magnet size was increased.

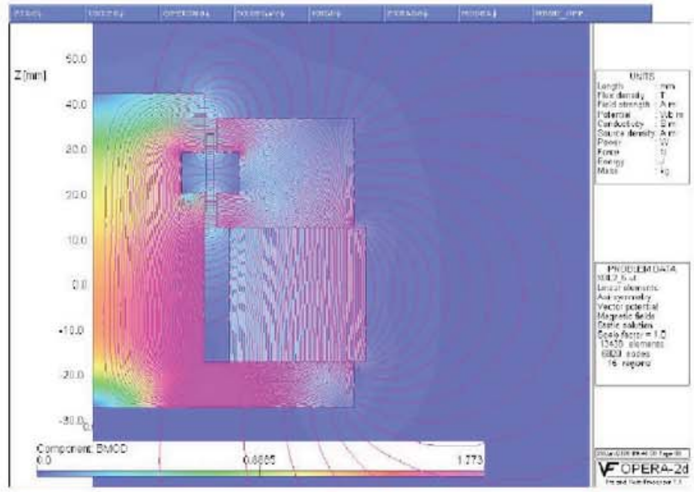

FIGURE 21: Contour plot of the simulation of the DC flux distribution for the SBL2 motor assembly model.

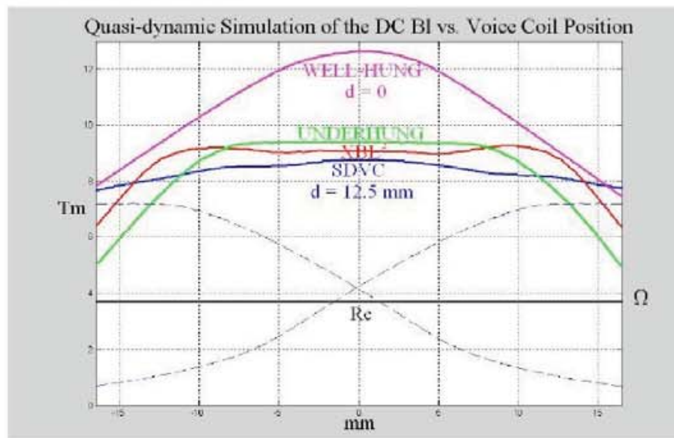

FIGURE 22: Plots of the simulations of B1(x) for the wellhung, underhung, XBL2, and SDVC voice coil and the respective motor assembly models.

ENGINEER'S COMMENTS

The SDVC is similar to the decade-old wellhung motor topology. It seems obvious now that the high peak Bl(0) could be traded for linear X_{max} but that was not the design criterion back in 1998-1999 and the Klippel DA was not widely available. One nice thing about the SDVC is that this topology is inherently very flexible with regard to target nonlinear design parameters and implementations. For a given gap height, it looks like the SDVC is the most linear with respect to displacement but at the price of peak Bl(0). This can be compensated for with increased magnet volume and motor redesigning. It is possible to get ruler flat Bl(x) functions over a very high peak-peak stroke with the SDVC topology.

The challenge now shifts to suspension design and implementation, where 10″ low-frequency transducers are expected to have $X_{max} \geq 25$mm (one way). For 8″ low-frequency transducers, $X_{max} \geq 20$mm is a reasonable target. Larger transducers can have larger X_{max} targets.

The spacing between coils within the SDVC topology is another degree of freedom for the transducer engineer/designer. My objective was to keep things as "equal" as possible while still considering my previous wellhung motor implementations. All four finite element models are identical at the OD and height dimensions. Only the gaps are different, and this is to accommodate the respective voice coil OD.

What I find intriguing is that the SDVC is the "dual" of XBL^2. The XBL^2 voice coil is underhung at the rest position but there are effectively two magnetic gaps; however, the coil when displaced from $x = 0$ is overhung with respect to each gap, whereas the SDVC is effectively overhung at the rest position with one gap and two coils. However, each coil is effectively underhung with regard to the single tall gap. At the end of the day, it's still just another way to trade small signal sensitivity for X_{max}.

I propose that transducer manufacturers and developers get a Klippel DA and evaluate the large signal behavior of their products and perhaps their competitors' products too, and then consider new product development options as indicated by the measurement results. Low distortion, high excursion motor/voice coil and suspension designs and implementation are essential to high-performance low-frequency transducers. ***VC***

Steve Mowry is president of S. M. Audio Engineering (www.s-m-audio.com). He has a BS degree in Business Administration from Bryant College and BS and MS degrees in Electrical Engineering with highest distinction from the University of Rhode Island. He has worked in loudspeaker R&D at BOSE, TC Sounds, EASTECH, and P.Audio. He was responsible for the design and development of BOSE's 2¾" plastic basket multimedia AM5/Lifestyle "cube" transducer in 1997-1998, "Hotshot." This in raw quantity is one of the largest selling electrodynamic audio transducers of all time and is still being manufactured today. Steve is currently an independent researcher, lecturer, and consultant in transducer/loudspeaker system design and new product development along with being a frequent contributor to *Voice Coil* and *Multi Media Manufacturer*.